UC San Diego

Learning to Correct Axial Motion in OCT for 3D Retinal Imaging

Presenter: Yiqian Wang

Authors: Yiqian Wang[1], Alexandra Warter[2], Melina Cavichini-Cordeiro[2], William R. Freeman[2], Dirk-Uwe G. Bartsch[2], Truong Q. Nguyen[1], Cheolhong An[1]*

[1] Electrical and Computer Engineering Department, UC San Diego

[2] Jacobs Retina Center, Shiley Eye Institute, UC San Diego

IEEE ICIP 2021

Outline

- **Introduction**
- **Related works**
- **OCT axial motion correction network**
  - Problem formulation
  - Network architecture
  - Loss functions
  - Ground truth and data augmentation
  - Experiment setting
  - Experimental results
- **Conclusion**

Optical coherence tomography (OCT)

- Non-invasive 3D imaging at µm resolution
- One of the most important imaging modality in ophthalmology
- Imaging based on interference with low coherent infrared beam
- **A-scan**: (Z axis) magnitude of backscattered light from different depths
- **B-scan**: (XZ plane) 2D cross-sectional image;
- **Z axis**: axial direction, fastest; **X axis**: fast scanning axis; **Y axis**: slow scanning axis

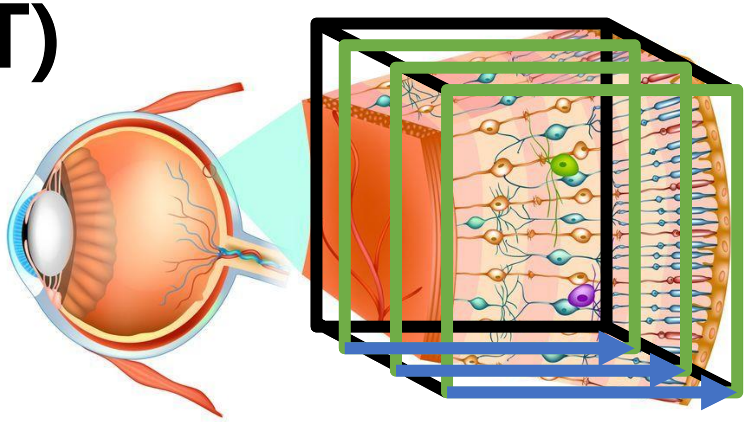

OCT imaging of the retina[1]

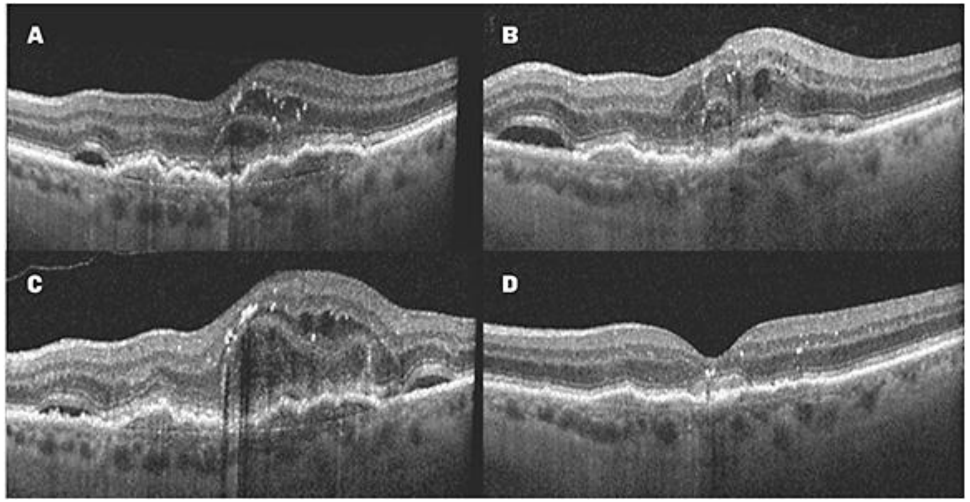

Cross-section view of retinal diseases using OCT[2]

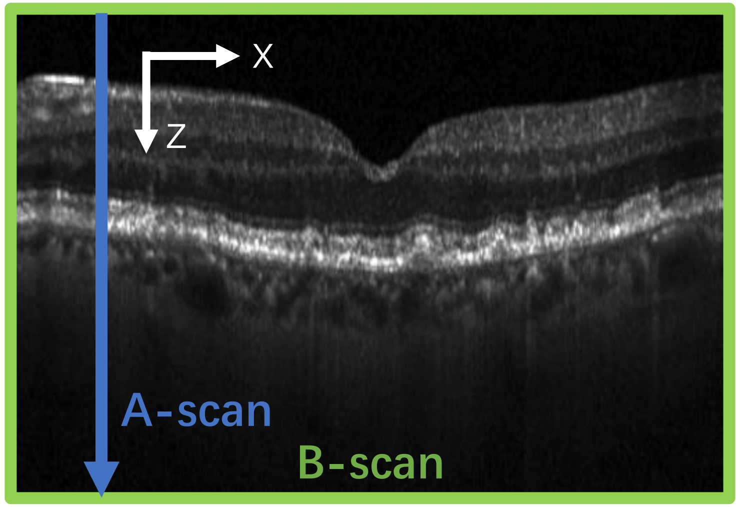

OCT A-scan (blue) and B-scan (green)

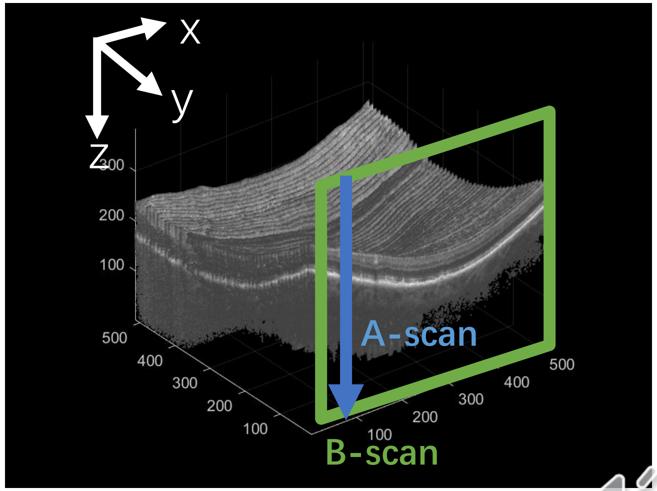

3D-OCT volume

UC San Diego

Motion artifacts

Motion artifacts in OCT compromise 3D visualization and subsequent processing

Sources of involuntary motion

- Tremors: 25–90 Hz, amplitude 8.5” (6 µm)
- Drifts: 6’/s to 30’/s, amplitude 0.8’-31.4’
- Microsaccades: fastest and largest
- Pulsing and Respiration: amplitude of 81±3.5µm

Axial motion artifacts in OCT

- Cause discontinuities of neighboring B-scans in the slow scanning axis

Coronal motion artifacts in OCT

- Cause distortion of vessels in the en-face image (XY plane)
- Smaller range compared with axial motion

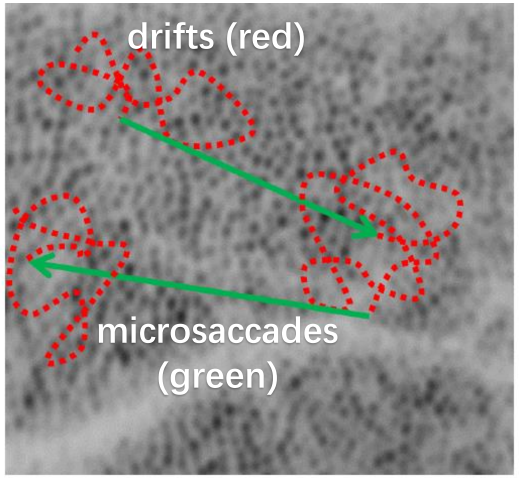

Schematic of eye motion[3]

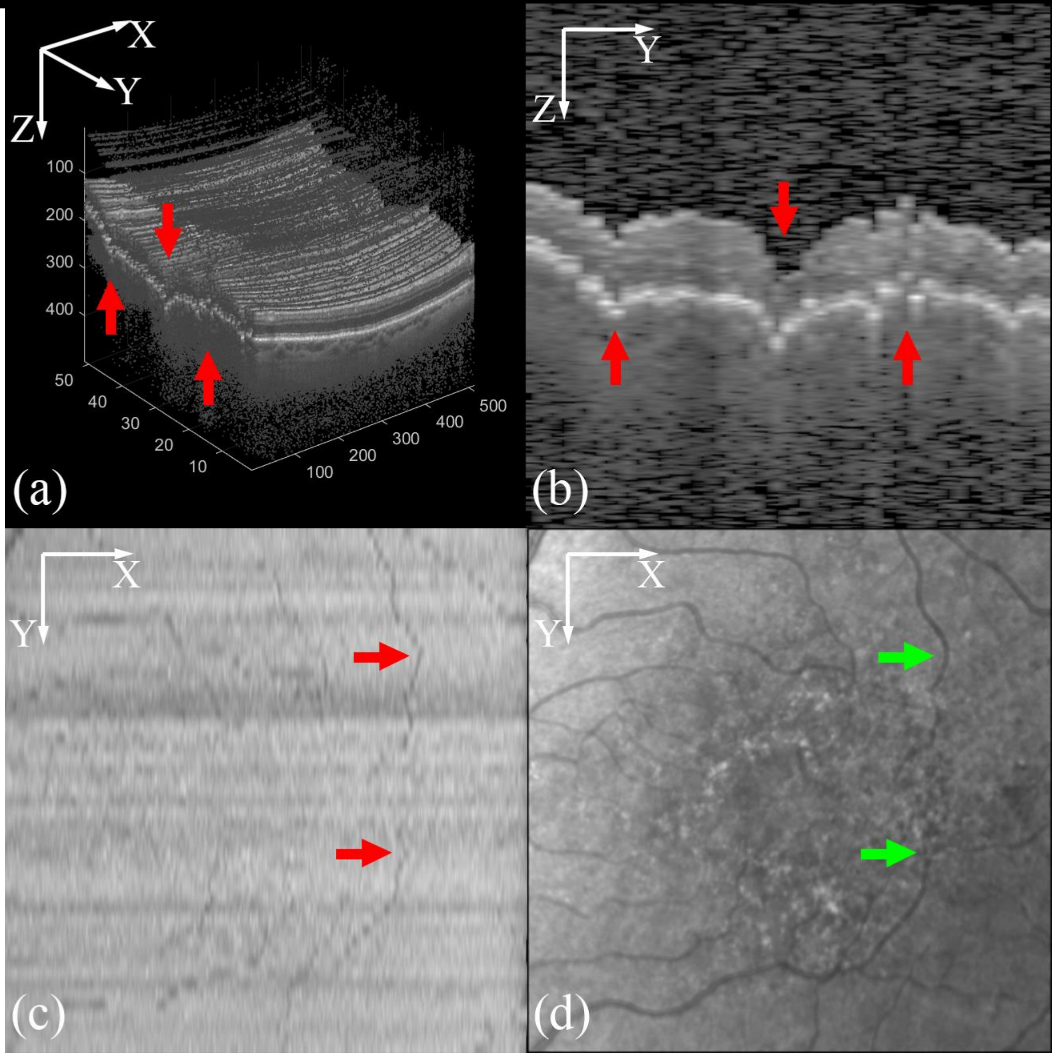

Motion artifacts in OCT
(a) Axial motion in 3D, (b) axial motion in cross-sectional B-scan
(c) coronal motion in en-face C-scan, (d) reference infrared image

[3] Brea et al. “Review on Retrospective Procedures to Correct Retinal Motion Artefacts in OCT Imaging”, Appl. Sci, 2019

Outline

- Introduction
- Related works
- **OCT axial motion correction network**
  - Problem formulation
  - Network architecture
  - Loss functions
  - Ground truth and data augmentation
  - Experiment setting
  - Experimental results
- **Conclusion**

UC San Diego

Related works in OCT motion correction

Prospective (hardware-based) methods

- Additional hardware mounted onto the OCT scanner
- Eye tracking hardware to track motion during OCT data acquisition
- Depend on special scanning patterns (e.g. dual beam)
- Require special signal acquisition techniques

Retrospective (software-based) methods

- Post-processing after OCT acquisition
- The only option for imaging systems without eye tracking hardware
- Estimate eye motion from a single or multiple OCT volumes
- Apply inter-frame image registration techniques

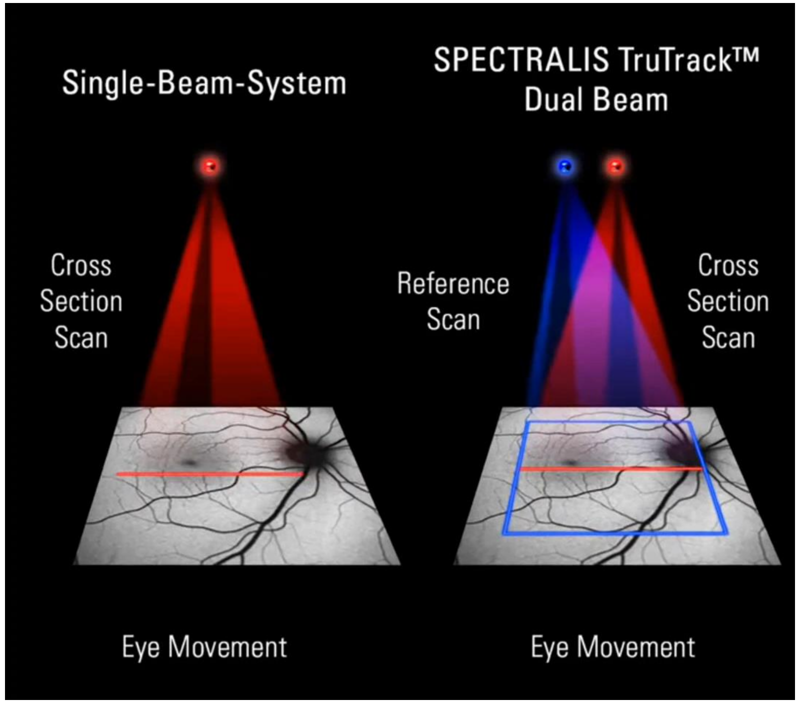

Heidelberg Spectralis TruTrack eye tracking system [4]

[4] Heidelberg Engineering, https://business-lounge.heidelbergengineering.com/gb/en/products/spectralis/

UC San Diego

Related works – retrospective approaches

Scope	Multiple OCT volumes	Single OCT volume
Axial motion only	**Potsaid et al. 2008 [5]** Orthogonal reference scans to the slow axis + Effectively corrects axial motion, recover curvature - Time consuming to capture multiple scans	**Antony et al. 2011 [6]** Retinal layer segmentation, TPS fitting - Prone to segmentation error - Flattens RPE surface, bad for observing diseases **Proposed** axial motion correction network
Axial + coronal motion	**Kraus et al. 2012 [7] and 2014 [8]** Corrects motion via registration of orthogonal volumes + Standard tool for OCT-A preprocessing - Time consuming to capture multiple scans + Works well for dense OCT scans (496×512×512) - Not desirable for sparse OCT scans (496×512×49)	**Montuoro et al. 2014 [9]** Retinal layer segmentation, local symmetry - Prone to segmentation error - Assumption does not hold for retinal diseases **Fu et al. 2016 [10]** Based on saliency and correlation - Overly smoothed retina

Full references at the end of presentation

Outline

- Introduction
- Related works
- **OCT axial motion correction network**
    - Problem formulation
    - Network architecture
    - Loss functions
    - Ground truth and data augmentation
    - Experiment setting
    - Experimental results
- **Conclusion**

Problem formulation

Input: OCT volume **V**, H×W×N

- H: Height of B-scans, Z axis, axial direction
- W: Width of B-scans, X axis, fast-scanning direction
- N: Number of B-scans, Y axis, slow-scanning direction

Output: 2D displacement map **D**, W×N

- Negative: Shifts column upwards
- Positive: Shifts column downwards
- Magnitude: Number of pixels divided by a normalization factor Z_{norm}.

Final corrected OCT volume: $\mathbf{V}_{\text{out}}(z, x, y) = \mathbf{V}(z - Z_{\text{norm}}\mathbf{D}(x, y), x, y)$

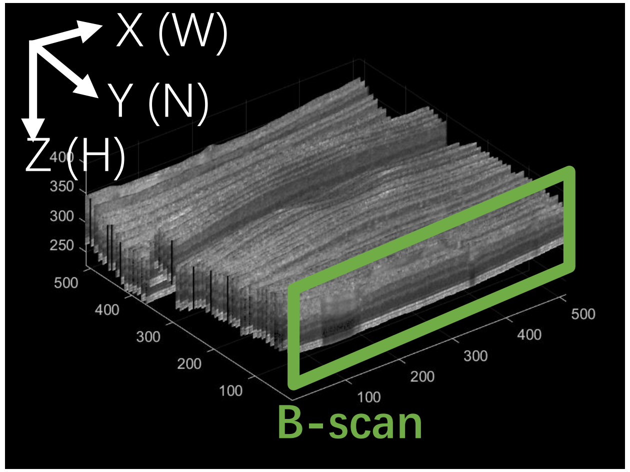

Input OCT volume

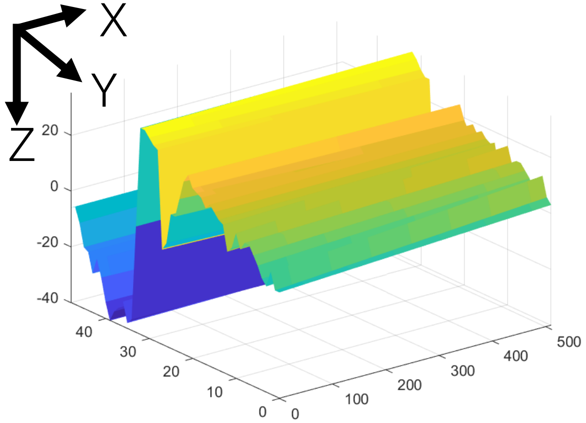

2D axial displacement map

Network architecture

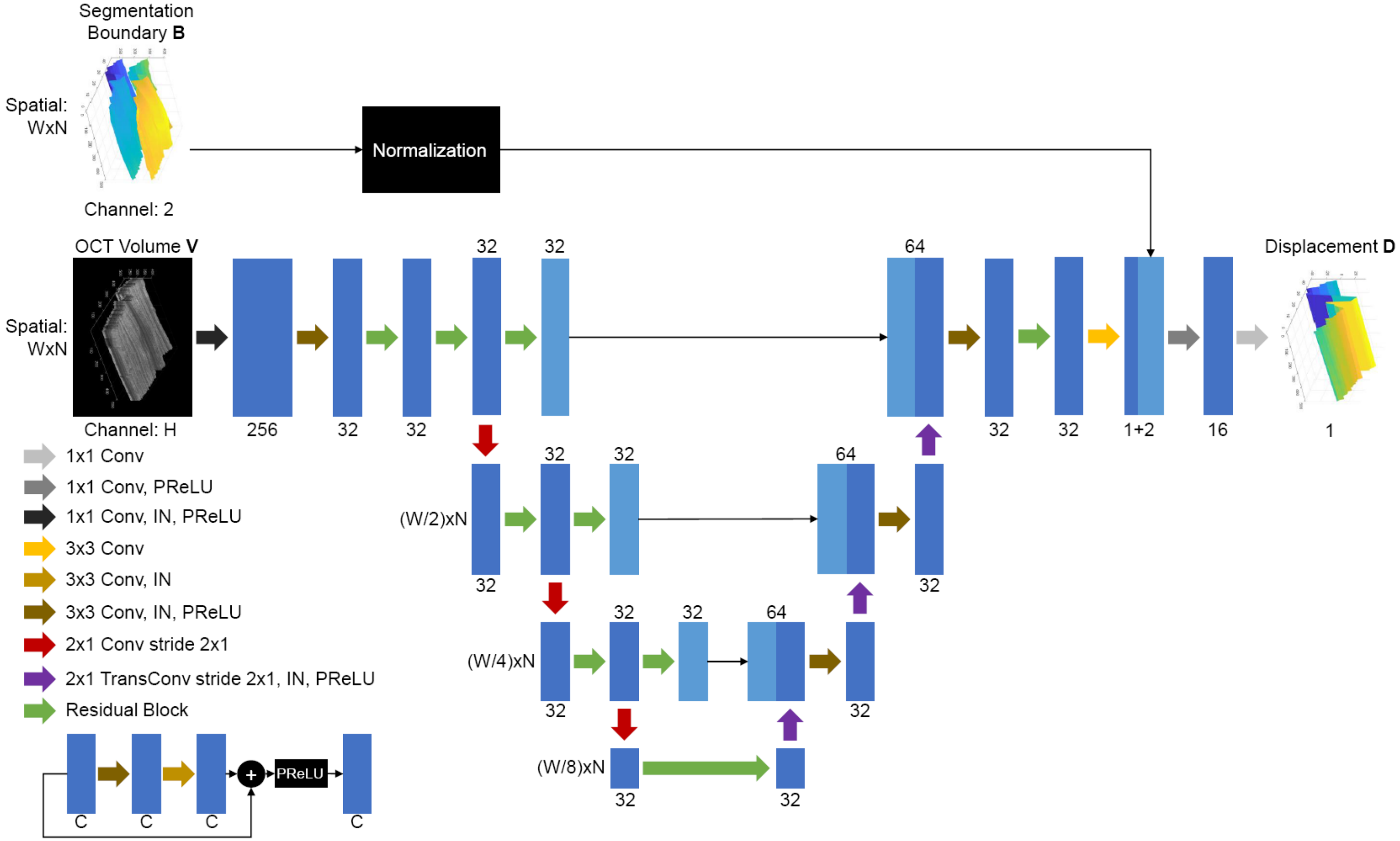

The OCT axial motion correction network

Architecture:

- Modified U-Net with residual blocks
- 1×1 convolution at the first layer to compress the number of channels
- Instance normalization (IN) applied after convolutions
- 2×1 convolution with stride 2×1 for multiresolution analysis
- Includes segmentation boundaries of the ILM and RPE layer of the retina

Advantages:

- Fully convolutional architecture
- Arbitrary number of stacked B-scans

UC San Diego

Ground truth and data augmentation

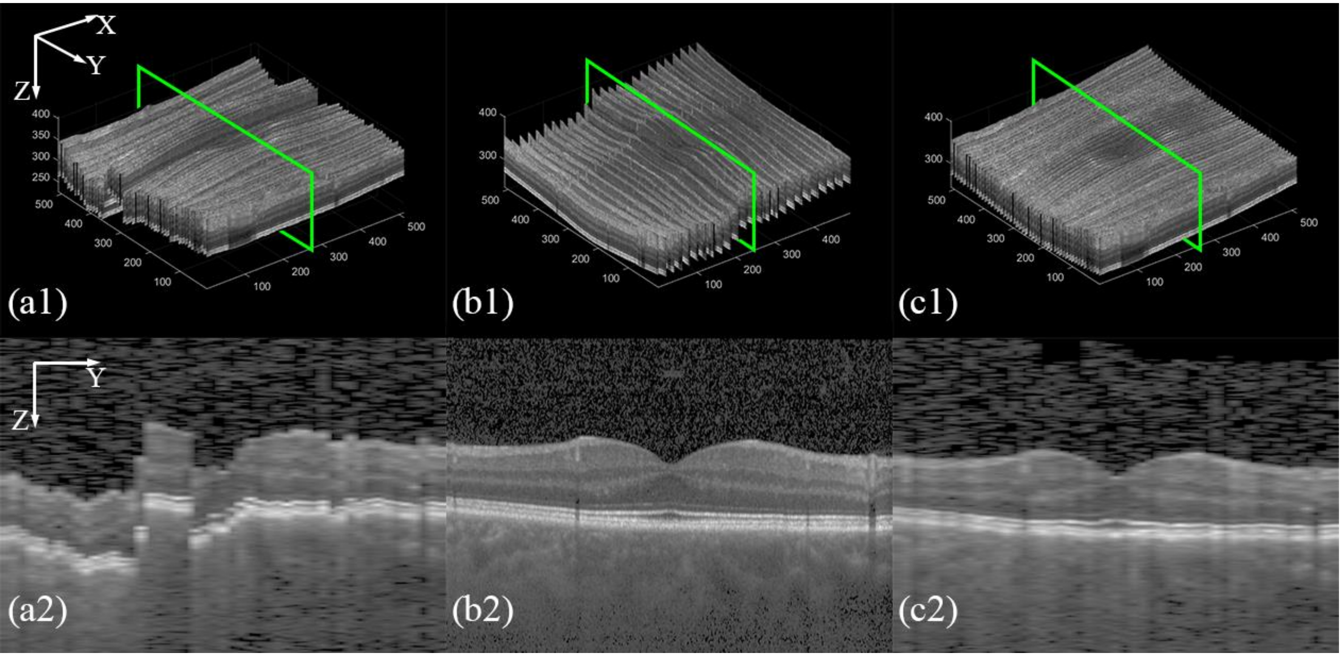

The orthogonal approach [5] for ground truth acquisition

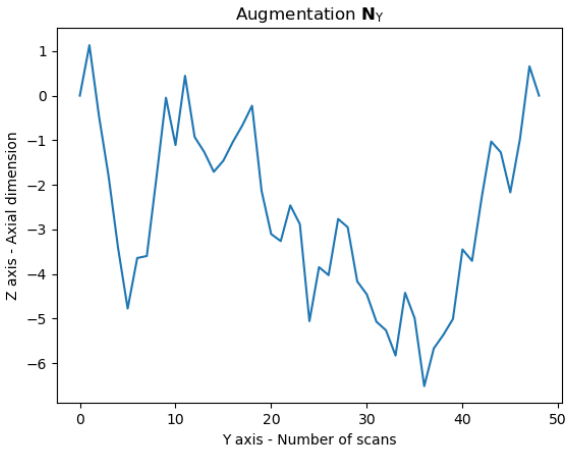

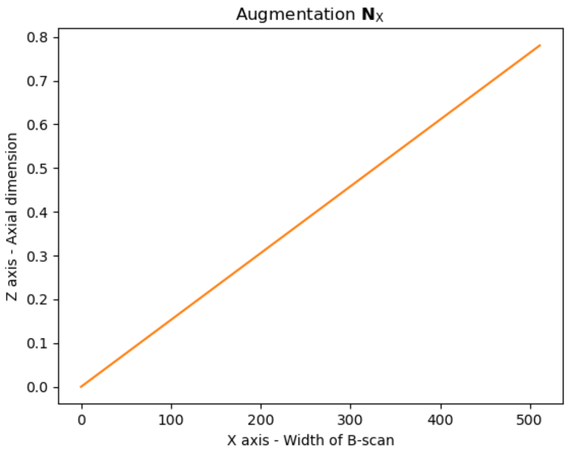

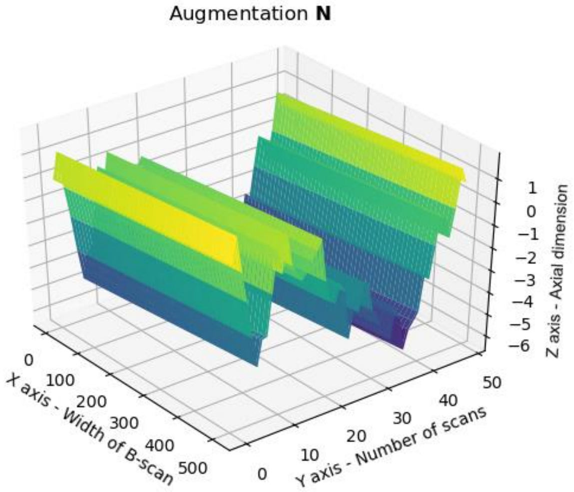

Data augmentation by adding random displacement to the Y axis, and random tilt to the X axis

[5] B. Potsaid, et al., "Ultrahigh speed spectral/fourier domain oct ophthalmic imaging at 70,000 to 312,500 axial scans per second," Optics express, 2008.

UC San Diego

Loss functions

L1 displacement Loss

$$\mathcal{L}_{\text{disp}}(\mathbf{D};\mathbf{D}_{\text{GT}}) = \underset{x,y}{\text{mean}}\left(\mathbf{M}(x,y)|\mathbf{D}(x,y) - \mathbf{D}_{\text{GT}}(x,y)|\right)$$

- Absolute difference between predicted and GT displacement
- Mask **M** to assign higher weight at the center

Mask applied to the L1 displacement loss

Smoothness loss

$$\mathcal{L}_{\text{smooth}}(\mathbf{D}) = \sum_{s=1,2} \underset{x,y}{\text{mean}}(|\mathbf{D}^s(x+1,y) - \mathbf{D}^s(x,y)|)$$

- Where $\mathbf{D}^1$ denotes the displacement at original resolution
- $\mathbf{D}^2$ denotes the displacement downscaled by 2 to the X axis.

Total loss

- Weighted combination of two loss terms: $\mathcal{L} = \mathcal{L}_{\text{disp}}(\mathbf{D};\mathbf{D}_{\text{GT}}) + \lambda_{\text{smooth}}\mathcal{L}_{\text{smooth}}(\mathbf{D})$

UC San Diego

Experiment setting

Dataset

- 110 (55 pairs of horizontal and vertical) OCT volumes
- Training, validation, test: 75, 10, 25 volumes
- Heidelberg Spectralis, imaging volume 1.9×5.8×5.8 mm^3
- Resolution 496×512×49 or 496×512×25
- Instrument segmentation boundaries of ILM, RPE

Post processing

- Least squares line fitting to the X axis
- Guarantees no distortion except shearing of fast B-scans

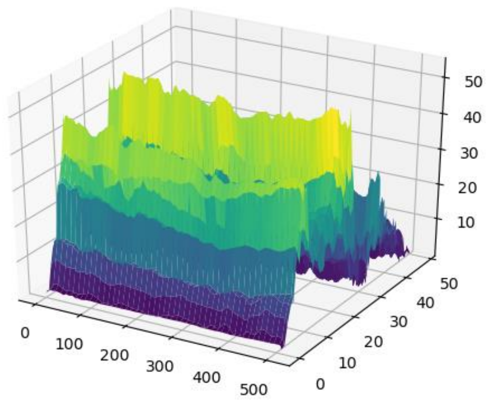

Predicted displacement map

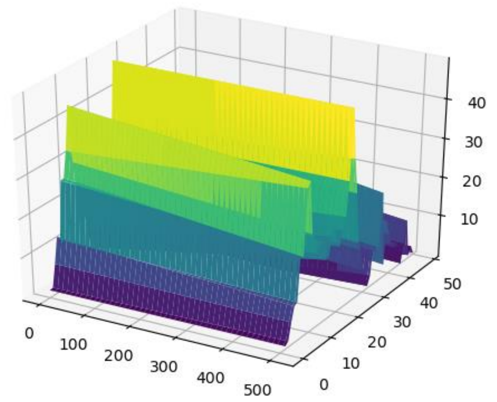

Displacement map after post processing

Experimental results

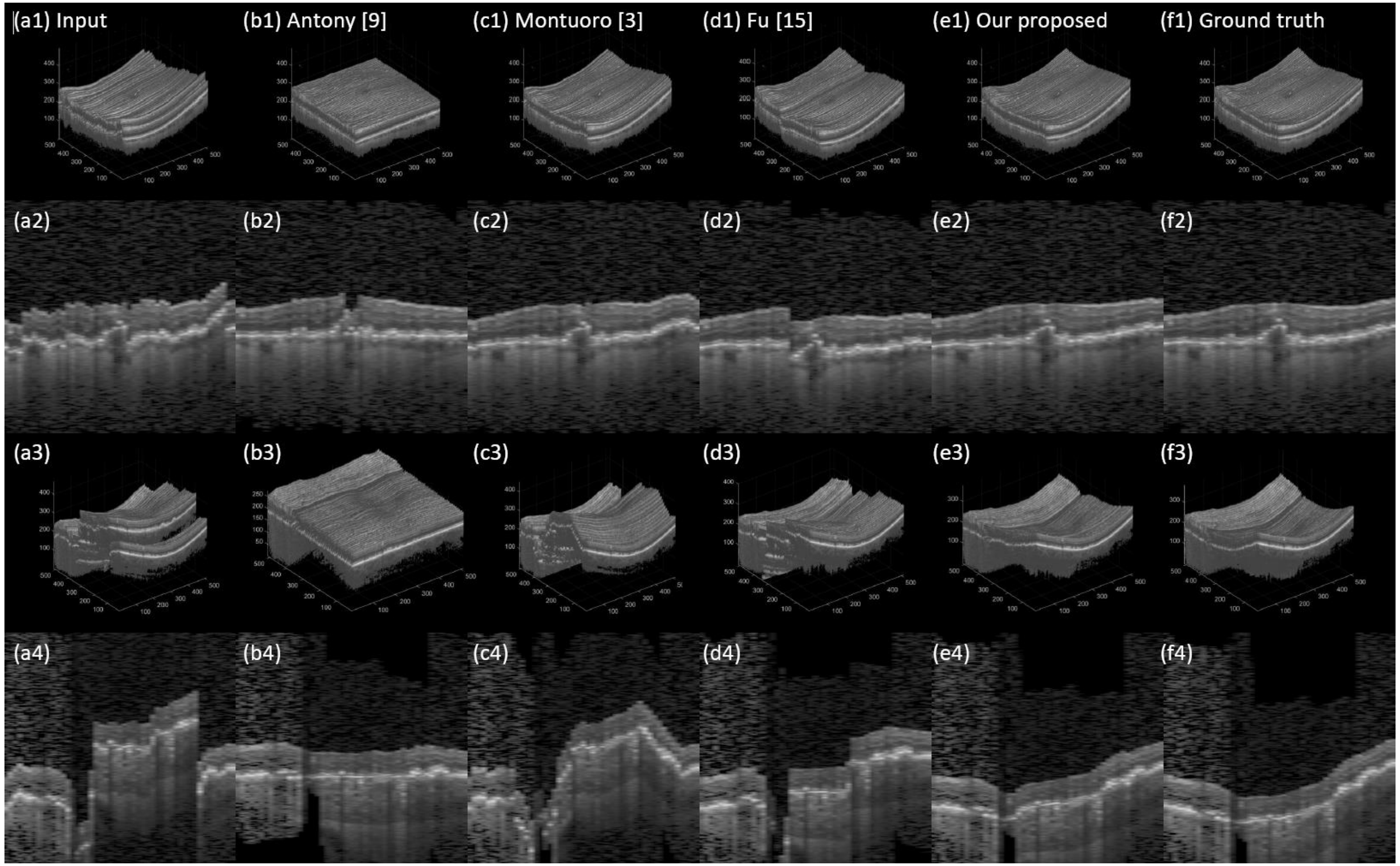

Qualitative result of different axial motion correction methods

Table 1: Quantitative result of axial motion correction

Method	MNMI	MAE
Before correction	0.5811 (±0.0219)	22.39 (±17.52)
Ground truth	0.5901 (±0.0200)	–
Antony et al	**0.5927 (±0.0190)**	28.28 (±10.63)
Montuoro et al	0.5831 (±0.0215)	20.28 (±16.35)
Fu et al	0.5922 (±0.0223)	26.94 (±14.49)
Our proposed	0.5898 (±0.0196)	**7.86 (±5.75)**

Evaluation metrics:

- **Smoothness:** mean normalized mutual information (MNMI, higher is smoother)
- **Overall error:** mean absolute error of displacement (MAE, smaller is better)

Discussion:

- Our method achieves the lowest MAE at 7.86 pixels, and the MNMI is close to the ground truth

Outline

- **Introduction**
- **Related works**
- **OCT axial motion correction network**
  - Problem formulation
  - Network architecture
  - Loss functions
  - Ground truth and data augmentation
  - Experiment setting
  - Experimental results
- **Conclusion**

Conclusion

- OCT motion artifacts severely compromise 3D visualization and analysis
- We proposed a fully convolutional neural network for OCT axial motion correction based on a single volume input
- The proposed method can correct large motion, while recovering the true curvature of retina
- Achieved significant improvements compared to conventional methods in normal and disease cases

Significance:

- Better display and visualization of 3D OCT volumes
- Benefit subsequent analysis including retinal layer segmentation and OCT-A imaging

Future work:

- Extend proposed network to support coronal motion correction besides axial motion

UC San Diego

Thank you!

"Learning to Correct Axial Motion in OCT for 3D Retinal Imaging"

Yiqian Wang

06/01/2021

References

UC San Diego

[1] L. Charters, "OCT: Illuminating the retina layer by layer," https://www.ophthalmologytimes.com/view/oct-illuminating-retina-layer-layer, July 12, 2021

[2] P. A. Karth, "Today's OCT platforms drive personalized AMD care", https://www.retinalphysician.com/supplements/2020/april-2020/oct-interpretation/today-8217;s-oct-platforms-drive-personalized-amd, July 12, 2021

[3] L. Sanchez Brea, D. Andrade De Jesus, M. F. Shirazi, M. Pircher, T. van Walsum, and S. Klein, "Review on retrospective procedures to correct retinal motion artefacts in oct imaging," Applied Sciences, vol. 9, no. 13, p. 2700, 2019.

[4] Heidelberg Engineering, "Spectralis", https://business-lounge.heidelbergengineering.com/gb/en/products/spectralis/, July 12, 2021

[5] B. Potsaid, I. Gorczynska, V. J. Srinivasan, Y. Chen, J. Jiang, A. Cable, and J. G. Fujimoto, "Ultrahigh speed spectral/fourier domain oct ophthalmic imaging at 70,000 to 312,500 axial scans per second," Optics express, vol. 16, no. 19, pp. 15149-15169, 2008.

[6] B. Antony, M. D. Abramoff, L. Tang, W. D. Ramdas, J. R. Vingerling, N. M. Jansonius, K. Lee, Y. H. Kwon, M. Sonka, and M. K. Garvin, "Automated 3-d method for the correction of axial artifacts in spectral-domain optical coherence tomography images," Biomedical optics express, vol. 2, no. 8, pp. 2403-2416, 2011.

[7] M. F. Kraus, B. Potsaid, M. A. Mayer, R. Bock, B. Baumann, J. J. Liu, J. Hornegger, and J. G. Fujimoto, \Motion correction in optical coherence tomography volumes on a per a-scan basis using orthogonal scan patterns," Biomedical optics express, vol. 3, no. 6, pp. 1182{1199, 2012.

[8] M. F. Kraus, J. J. Liu, J. Schottenhamml, C.-L. Chen, A. Budai, L. Branchini, T. Ko, H. Ishikawa, G. Wollstein, J. Schuman, et al., "Quantitative 3d-oct motion correction with tilt and illumination correction, robust similarity measure and regularization," Biomedical optics express, vol. 5, no. 8, pp. 2591-2613, 2014.

[9] A. Montuoro, J. Wu, S. Waldstein, B. Gerendas, G. Langs, C. Simader, and U. Schmidt-Erfurth, "Motion artefact correction in retinal optical coherence tomography using local symmetry," in International Conference on Medical Image Computing and Computer-Assisted Intervention, pp. 130-137, Springer, 2014.

[10] H. Fu, Y. Xu, D. W. K. Wong, and J. Liu, "Eye movement correction for 3d oct volume by using saliency and center bias constraint," in 2016 IEEE Region 10 Conference (TENCON), pp. 1536-1539, IEEE, 2016.